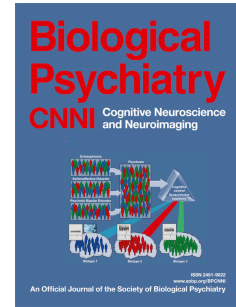


Accepted Manuscript

Associations of psychopathic traits with local and global brain network topology in young adult women

Philip Lindner, Pär Flodin, Meenal Budhiraja, Ivanka Savic, Jussi Jokinen, Jari Tiihonen, Sheilagh Hodgins



PII: S2451-9022(18)30104-6

DOI: [10.1016/j.bpsc.2018.04.010](https://doi.org/10.1016/j.bpsc.2018.04.010)

Reference: BPSC 282

To appear in: *Biological Psychiatry: Cognitive Neuroscience and Neuroimaging*

Received Date: 31 October 2017

Revised Date: 24 April 2018

Accepted Date: 25 April 2018

Please cite this article as: Lindner P., Flodin P., Budhiraja M., Savic I., Jokinen J., Tiihonen J. & Hodgins S., Associations of psychopathic traits with local and global brain network topology in young adult women, *Biological Psychiatry: Cognitive Neuroscience and Neuroimaging* (2018), doi: [10.1016/j.bpsc.2018.04.010](https://doi.org/10.1016/j.bpsc.2018.04.010).

This is a PDF file of an unedited manuscript that has been accepted for publication. As a service to our customers we are providing this early version of the manuscript. The manuscript will undergo copyediting, typesetting, and review of the resulting proof before it is published in its final form. Please note that during the production process errors may be discovered which could affect the content, and all legal disclaimers that apply to the journal pertain.

Associations of psychopathic traits with local and global brain network topology in young adult
women

Philip Lindner^{1,2,3*}

Pär Flodin^{1,4,5}

Meenal Budhiraja¹

Ivanka Savic^{6,7}

Jussi Jokinen^{1,8}

Jari Tiihonen^{1,9}

Sheilagh Hodgins^{1,10}

¹Department of Clinical Neuroscience, Karolinska Institutet, Stockholm, Sweden

²Department of Psychology, Stockholm University, Stockholm, Sweden

³Center for Dependency Disorders, Stockholm Health Care Services, Stockholm County Council,
Stockholm, Sweden

⁴Umeå Center for Functional Brain Imaging, Umeå University, Umeå, Sweden

⁵Center for Aging and Demographic Research, Umeå University, Umeå, Sweden

⁶Department of Women's and Children's Health, Karolinska Institutet, Stockholm, Sweden

⁷Neurology Clinic, Karolinska University Hospital, Huddinge, Sweden

⁸Department of Clinical Sciences, Umeå University, Umeå, Sweden

⁹Department of Forensic Psychiatry, University of Eastern Finland, Niuvanniemi Hospital,
Kuopio, Finland

¹⁰Département de Psychiatrie, Université de Montréal, Montréal, QC, Canada

***Corresponding author:**

eStöd, Riddargatan 1, Stockholm, 114 35, Stockholm

philip.lindner@ki.se

+46 70 452 25 87

Word count, abstract: 249

Word count, main text: 4172

Number of tables: 2

Number of figures: 5

Supplementary material: Two sections, three tables and one figure

Abstract

Background: Psychopathic traits vary dimensionally in the population and are associated with multiple negative outcomes. The Impaired Integration Theory (IIT) proposes that psychopathic traits are associated with abnormal neural network topology, such that disturbed integration of neural networks results in a self-perpetuating impairment in rapid integration and learning from multiple components of information. The IIT is based on findings from male offenders presenting high scores on all psychopathic traits. The present study investigated whether IIT predictions of topology abnormalities were associated with psychopathic traits, measured dimensionally, in young adult women with sub-syndromal scores.

Methods: 73 women, aged, on average, 25 years, were assessed using the Psychopathy Checklist-Revised and completed resting-state Magnetic Resonance Imaging. Preprocessed time-series from 90 anatomical regions were extracted to form connectivity matrices and used to calculate network topology based on graph theory. Correlations between total psychopathy and factor scores with both the raw connectivity matrix and global and local graph theory measures were computed.

Results: Total psychopathy scores and behavioral factor scores were related to connectivity between several pairs of regions, primarily limbic/paralimbic. Psychopathic traits were not associated with global topology measures. Topology abnormalities, robust across network formation thresholds, were found in nodes of the Default Mode Network, and in hubs connecting several resting-state networks.

Conclusions: IIT predictions of abnormal topology of hubs and Default Mode Network nodes with dimensionally measured psychopathic traits were confirmed in a sample of young women. Regional abnormalities, accompanied by preserved global topology, may underlie context-specific abnormal information processing and integration.

Keywords: Graph theory | Psychopathy | Topology | Connectivity | Resting-state | Default Mode Network

Introduction

Psychopathic traits include stable patterns of behaviors, such as antisocial behavior, impulsivity, and sensation-seeking, and of personality, such as callousness, lack of guilt and empathy, grandiosity, and a capacity to manipulate others (1). The behavioral traits, referred to as the Social Deviance factor of psychopathy, index symptoms similar to the diagnosis of Conduct Disorder (CD) in childhood and Antisocial Personality Disorder (ASPD) in adulthood. By contrast, the personality traits, referred to as the Interpersonal-Affective factor, are unique to psychopathy. Psychopathic traits vary dimensionally in the population (2), emerge early in life (3), remain relatively stable from early to late childhood (4), and from adolescence into early adulthood (5), predict a wide range of adverse outcomes, including criminal offending, limited academic achievement, unemployment, and mental disorders (4–7), and are highly heritable (8–11). Females present lower levels of psychopathic traits than males (12–14), and a somewhat different phenotype with less physical aggression (15).

Further understanding of the neural abnormalities associated with psychopathic traits is needed to inform interventions. Most brain research on psychopathy has been conducted with incarcerated male offenders, comparing those who do, and who do not, present the syndrome of psychopathy, defined as high scores on both the behavioral and personality factors. Structural and functional abnormalities have been reported in the amygdala, orbitofrontal cortex (OFC), insula, hippocampus, and (16–18) some evidence of sex differences (19, 20) However, these findings fail to explain the breadth and contextual specificity of both cognitive and affective abnormalities associated with psychopathy. Recently, the Impaired Integration Theory (IIT) proposed that psychopathy is a disorder of disturbed integration of neural networks, resulting in a self-perpetuating impaired ability to rapidly integrate distinct bits of information necessary for contextual and operant learning (21). The IIT attempts, for the first time, to integrate findings of attentional bottlenecks, reduced affective empathy, and difficulty in passive avoidance learning, with structural and functional brain abnormalities that have been observed among male offenders with high psychopathy scores (21).

Few studies have tested the predictions of the IIT, and none have determined whether aberrant network topology is associated with psychopathic trait scores in women. Investigating regional resting-state activity abnormalities within specific networks using techniques such as independent component analysis and seed region analysis does not test hypotheses regarding network topology. However, using graph theory, abnormalities associated with psychopathic traits can be investigated at a network level as proposed by the IIT. Graph theory models the brain as a collection of nodes (grey matter regions), connected by edges, defined as either anatomical white matter connections (structural connectomics) or as correlations, either of activity over time (functional connectomics) or of a structural measure, like cortical thickness (22). Together, nodes and edges form a specific network topology, wherein some nodes are less connected than others (connection strength and number of edges, degrees) and more central to other nodes, forming the basis for higher-order topology measures such as betweenness centrality and efficiency. Topology measures may thus describe both local (node) and global (entire network) properties. See Table 1. Nodes with high degrees of betweenness centrality, and efficiency are referred to as hubs and serve to connect several subnetworks. Since neural information processing relies on exchanging information across nodes and subnetworks, abnormal network topology, particular of hub regions connecting subnetworks, is indicative of abnormal information processing (23). Brain topology has been associated with cognitive abilities such as working-memory (24), spatial orientation (25), personality traits (26) and intelligence (27).

The IIT predicts that high psychopathy scores are associated with reduced efficiency and increased modularity, at a global network level, with weaker long-range connections between different subnetworks and stronger connections within subnetworks. Key among implicated subnetworks are the frontoparietal control network (FpCN), cingulo-opercular network (CoN), ventral attention network (VAN), default mode network (DMN) and salience network (SAN) (21). Together, these networks enable higher-order cognition and behavior through associative processing, impairments of which may promote psychopathic traits. The presence of global

network abnormalities signals abnormal local (node) network properties, although not necessarily vice versa. Three studies (28–30) have employed graph theory to model network topology in antisocial individuals. Two of these studies modeled gray matter structural topology (28, 29) and one resting-state functional topology (30). Altered modular organization and impaired network efficiency were found to characterize both adolescents with CD (29), and adult males with ASPD (30) and psychopathy (28), while findings on clustering coefficients and characteristic path length were inconsistent across studies (28, 30). Congruently, several studies of antisocial adults and adolescents have reported abnormal structural integrity of the corpus callosum (31–35) that enables interhemispheric connectivity, of the uncinate fasciculus (20, 33, 36–44) that enables amygdala-OFC connectivity; and more widespread abnormalities in white matter integrity (31, 33, 40, 45–47).

The IIT was based on studies of incarcerated male offenders with the syndrome of psychopathy, and the subsequent graph theory studies focused on males diagnosed with CD (29) or ASPD (28, 30). However, accumulating evidence indicates that psychopathic traits measured dimensionally may be more meaningfully associated with neural abnormalities than a category defined by a high cut-off score (48). Presently, it is not known whether the IIT applies to psychopathic traits measured dimensionally in individuals not presenting the syndrome of psychopathy. Additionally, it is not known whether the IIT applies to females. From an early age and onwards, females present higher within-subnetwork functional (49) and between-hemisphere structural (50) connectivity than males who males present higher between-subnetwork functional connectivity (49). Since both the phenotype and connectivity differ in males and females, findings and predictions from studies of males may not generalize to females. The present study investigated resting-state network topology in young women. We predicted that consistent with the IIT, total psychopathic traits, and factor scores, would be associated with impaired functional connectivity between nodes of different networks, especially interhemispheric networks, and increased connectivity between nodes within the same network, manifesting as reduced global efficiency and increased clustering coefficient, and

reduced topological integration in key regional hubs common to several different networks. Unlike previous studies, we took account of comorbid disorders known to have increased prevalence among individuals with elevated psychopathy scores (51–53), each of which is independently associated with resting-state abnormalities (54–56).

Methods and Materials

The current study, and previous waves of data collection, were approved by the Regional Ethical Review Board (*Etikprövningsnämnden*), in Stockholm. Participants provided written informed consent. For the present study, participants received 1600 SEK in gift certificates.

Participants

Participants were recruited from a prospective, longitudinal study of individuals who sought treatment for substance misuse in adolescence (34, 57–61). The sample for the present study included all 43 ex-clients of the clinic and 30 sisters of ex-clients for whom high-quality fMRI data were available. Psychopathy had been assessed approximately 18 months prior to scan. The mean age of participants at time of scan was 24.6 (SD=3.2) years.

Procedure

Potential participants were contacted by telephone and mail and invited to take part in an additional follow-up assessment (34).

Clinical assessment

Prior to scan, participants completed the Structured Clinical Interview for DSM-IV Axis I Disorders (SCID) (62). Current alcohol dependence, drug dependence, depression and any anxiety disorder were considered possible clinical confounders. Current psychoactive medication was self-reported. Verbal and performance intelligence (VIQ and PIQ) were assessed at a prior assessment. Table S1 presents sample characteristics, and Table S2 associations of IQ and comorbid disorders with psychopathy scores.

Psychopathy assessment

Psychopathic traits were assessed using the Psychopathy Checklist Revised (PCL-R) (1) by a trained assessor approximately 18 months prior to scan. All available information collected

on the same occasion (e.g. mental disorders, self-reported delinquency, psychosocial functioning) was used to rate items. Mean scores were low: total 5.22 (SD=5.40, range: 0-25); factor 1 1.70 (SD=2.34, range: 0-11); factor 2 mean 3.16 (SD=3.20, range=0-14). Figure 1 presents distributions of scores. The two factor scores were strongly correlated ($r=.76$, $p<.001$) as would be expected (63). One participant obtained a total score ≥ 25 , the commonly used European cut-off (64). In the present study, total scores for psychopathic traits, and for each factor, were examined. Inter-rater reliability of PCL-R scores was assessed in the larger sample from which participants were drawn (5). Intraclass correlation coefficients were high: total score 0.99; interpersonal facet 0.79; affective facet 0.85; lifestyle facet 0.82; and antisocial facet 0.97. As presented in Figure S1, confirmatory factor analysis showed that the four-facet solution typically found in offender samples was a good fit to the data, with somewhat lower loadings of some items, and that facets 3 and 4 were not as strongly correlated with each other as with facets 1 and 2.

MRI acquisition and preprocessing

Resting-state fMRI data were acquired on a 3-Tesla GE MR750 scanner with the following parameters: flip angle, 90°; repetition time, 2.5 s, echo time, 30 ms; field of view, 288 mm²; slice thickness, 3 mm. During resting-state fMRI acquisition, participants were instructed to stay awake and focus on a white crosshair on a black background, viewable via a mirror. This procedure was employed to minimize fatigue and sleep. Functional and additional high-resolution structural data were preprocessed and analyzed using the CONN toolbox (65), running on SPM12 and Matlab14a; see Supplementary material for details. Seed regions were defined according to the 3mm, 90-region Automated Anatomical Labeling (AAL) atlas (66). Time series were extracted from each region and used to compute individual inter-region correlation matrices.

Analyses

All connectivity analyses were conducted using the GraphVar (version 1.02) software (67). First, correlations between psychopathy scores and inter-region connectivity were

investigated, since this connectivity forms the basis for higher-order network approaches, such as graph theory topology. For this purpose, 90×90 region connectivity matrices (r to z-transformed) were computed using time series extracted from all atlas regions. Because there is no consensus on how to interpret negative correlations between neural nodes (68), all negative correlations were set to zero. Matrix values were initially correlated with psychopathy total scores, then with factor 1 and 2 scores in separate multiple regression models. False Discovery Rate (FDR) was applied to correct for multiple comparisons. VIQ, PIQ (continuous variables), psychoactive medication at scan, and current mental disorders (dichotomous variables) were included in all statistical models as nuisance variables such that the associated variance was regressed out prior to the principal analyses.

Second, the inter-region matrices were used to compute network topology. Several local and global network topology indices, all weighted and undirected, were computed and correlated with psychopathy factor scores. These included both basic node topology measures such as degrees (number of edges of a certain node) and strength (summed strength of those edges), a measure of centrality in the network (betweenness, i.e. fraction of all shortest path that pass through the node), network integration (efficiency, i.e. the inverse shortest path length) and segregation (clustering coefficient, i.e. the fraction of the node's neighbors that are also neighbors of each other, and modularity). See Table 1 for details. Since there is no consensus on the appropriate range of connection strength thresholds to apply to network formation (68), we applied multiple thresholds of 0.2-0.5 (steps of 0.1) and considered only findings that were significant across two thresholds to be robust and of interest. Non-thresholded associations were also examined for all measures, both global and local, with the exception of node degree, since this measure does not make sense in a fully connected network.

The global network was constructed to include all 90 regions. As in the connectivity matrix analyses, negative correlations were set to zero. Local network topology was investigated in a subset of regions-of-interest (ROIs) within the larger global network. This subset consisted of key regions implicated in the five neural networks central to the IIT, of which four (bilateral

precuneus, insula, inferior tempoparietal junction (IPL) and anterior cingulate cortex (ACC)) constituted hubs, connecting several networks (21, 23). Other ROIs included the hippocampus, angular gyrus, medial prefrontal cortex (mPFC), and posterior cingulate cortex (PCC) (default mode network), and thalamus (cingulopercular network), ventrolateral PFC (vlPFC) (salience network), middle frontal gyrus (MFG) and ventrolateral PFC (vlPFC) (frontoparietal network), and TPJ (ventral attention network). See Table S3 for corresponding AAL ROIs. In the proposed ROI topology (Figure 2), all nodes within the same subnetwork were assumed to be inter-connected, and all hubs (defined as regions implicated in several networks and consistent with empirical reports (23, 69) were assumed to be inter-connected. Regression analyses estimated associations of network measures (both global and local) with total psychopathy and factor scores in separate models, adjusted for confounders as above.

Results

Inter-region connectivity

As presented in Table 2 and Figure 3, positive associations between connectivity of intra- and inter-hemispheric regions and total psychopathy scores were detected involving primarily limbic and paralimbic structures. Social Deviance factor scores were positively associated with connectivity of the left SMA with left and right rectus. There were no independent associations with the Interpersonal-Affective factor.

Global network topology

As illustrated in Figure 4, regardless of the network formation threshold (including non-thresholded formation), there were no significant associations between any global network topology measure and psychopathy total and factor scores.

Local network topology

As presented in Figure 5, total psychopathy scores were negatively associated with the strength of the left IPL and positively associated with betweenness of the right IPL. The latter was significant also in a non-thresholded network. Total psychopathy scores were also negatively associated with efficiency of the right angular gyrus. Interpersonal-Affective scores

were positively associated with right insula and right hippocampus betweenness, both of which were significant also in a non-thresholded network.

Discussion

The IIT is the first theoretical model to integrate diverse abnormalities presented by adult male offenders presenting the syndrome of psychopathy. If the IIT is found to be a valid model of psychopathic dysfunction, across different populations or in specific populations, it would suggest novel therapeutic interventions focused on remediating impaired processing and integration of multi-components of information across the brain, using, for example, cognitive training (70). We hypothesized that if the theory is correct, it would also apply to females and to neural correlates of psychopathic traits lower than those denoting the syndrome psychopathy. Psychopathic trait scores, like the syndrome, are associated with similar, but less severe, multiple, negative outcomes (6) and with similar abnormalities of brain structures and functioning (19, 42, 61, 71). Using graph theory to model the functional connectome (22), we identified several regional connectivity and local network abnormalities associated with psychopathy total and factor scores. However, psychopathy scores were not associated with any global network topology metric.

The pattern of results is complex, yet provides initial, partial, support for the IIT. Four common graph theoretical network measures were studied at a local level: degree (number of edges of a node), strength (sum of weighted edges), betweenness centrality (fraction of shortest paths in the network that pass through the node) and efficiency (inverse shortest path length). Associations were detected between psychopathic trait scores and topology measures in structures related to the DMN, the most prominent resting-state network. The Social Deviance factor score was positively associated with the right hippocampal betweenness, and the total psychopathy score was negatively associated with angular gyrus efficiency. These findings indicate that psychopathic traits were associated with the functional organization of the DMN, consistent with reports from several studies of DMN activity (44, 72) and DMN inter-regional functional connectivity (73) in antisocial adults and adolescents. Abnormalities of the DMN have

been associated with many mental disorders (74). The DMN is most active during rest and partially deactivates when engaged in an externally focused task (75). Recent studies of male offenders presenting the syndrome of psychopathy (76), and of males with autism (77), suggest that attenuated task-induced deactivation of the DMN, especially in orbitofrontal regions, is associated with socio-affective deficits. This attenuated deactivation may also promote interference with task-positive networks during goal-directed action, leading to impaired performance and instrumental learning (74), as proposed by the IIT.

Intriguingly, betweenness centrality of the right hippocampus was positively associated with the Interpersonal-Affective factor, and there was a trend ($p < .10$) towards it being negatively associated with the Social Deviance factor. Since the associations of the two psychopathy factors with betweenness centrality of the right hippocampus were in the opposite direction, the association with the total psychopathy scores was insignificant. Such suppression effects have previously been reported in several task-fMRI studies. In previous studies of antisocial adolescents (78, 79) and a community sample of adults (80) amygdala activity in response to emotional stimuli was positively associated with Social Deviance traits, and negatively associated with Interpersonal-Affective traits. Higher betweenness centrality indicates that more information flows through this node. However, in the present study, as no task was presented during the scan, the role of this network feature as it relates to psychopathy traits cannot be inferred. Abnormalities of the size and structure of the hippocampus have primarily been associated with Interpersonal-Affective traits in male offenders (81, 82). In addition, reduced activation of the hippocampus during both hot and cool executive function tasks has been observed in antisocial adolescents relative to healthy peers (83). In accordance with the IIT and the crucial role of the hippocampus in conditioning, hippocampal abnormalities likely promote the passive avoidance (84) and reversal learning impairments (85) associated with psychopathic traits.

We found abnormal topology in two of the investigated hub regions, the bilateral IPL and right insula, which connect several resting-state networks. Psychopathy total scores were

negatively associated with strength, and at a trend level also degree, of the left IPL and positively with right IPL betweenness centrality. The IPL region is involved in the default mode, cingulo-opercular and frontoparietal control networks. Although our study investigated correlations between regions rather than networks, lower degrees and connection strength of the left IPL hub can be parsimoniously interpreted as attenuated connectivity between different neural networks, as suggested by the IIT. If so, the increased betweenness centrality of the right IPL may reflect a compensatory mechanism manifested only in a higher-order network measure consistent with the absence of global topology abnormalities and with the IIT prediction that psychopathy is associated with abnormal, rather than impaired, topology (21), such that individuals scoring high on psychopathic traits rely on different processing circuits for specific tasks, yet achieve similar success with the task (91). Future studies featuring independent component analysis to distinguish connectivity within and between different resting-state networks, and during tasks, will be required to test these hypotheses.

We found that betweenness centrality of the right insula was positively associated with Interpersonal-Affective scores. Previous studies of antisocial children and adolescents have identified reduced insula volume (86) and reduced activation during executive function hot and cool tasks and during emotional processing (83). Male offenders presenting the syndrome of psychopathy are characterized by smaller insula volumes (87, 88), as well as reduced insula activity during aversive conditioning (89), and increased insula activity during empathy-eliciting tasks (90) and punished reversal learning trials (91). Although implicated in a range of higher- and lower-order functions including empathy, pain, and uncertainty, it has been proposed that the function of the insula cortex is to integrate and evaluate external and internal information as well as making and responding to predictions (69, 92). While finding insula topology abnormalities fits well with the IIT, we would expect to find *negative*, rather than positive associations between psychopathic traits and betweenness centrality. However, the increased betweenness centrality may reflect another compensatory mechanism to accommodate the abnormal functional organization, as manifested in abnormal topology of other nodes. Future

research focusing on hub connectivity, including tasks that deactivate the resting-state networks to allow specific information processing, will be required to draw more definite conclusions.

As noted, the IIT was based on findings from male offenders presenting the syndrome of psychopathy. The current study examined the applicability of the IIT to females who presented much lower levels of psychopathic traits. Consistent with previous evidence that lower levels of psychopathic traits were linearly related to structural and functional neural abnormalities (19, 42, 61, 71), our findings suggest that at least some of the hypothesized topology abnormalities are also linearly associated with psychopathic trait scores in females. Results inconsistent with IIT predictions may be explained by threshold effects wherein topology abnormalities are presented only above a certain threshold, even though taxometric analyses failed to identify such a severity threshold (2). Alternatively, or in combination, topology abnormalities may indeed be linearly associated with trait severity, but on a circuit level rather than node level (i.e. higher trait scores associated with more abnormalities of more circuits rather than with properties of individual nodes). The fact that we found no associations between trait severity and global topology does however contradict this account. Importantly, the present study cannot determine whether results inconsistent with the IIT are due to sex, low levels of psychopathic traits, or both. Future research is needed to clarify how topology abnormalities are associated with a wide range of psychopathic traits.

In order to aid interpretability of graph theory results, we also investigated associations between region-to-region connectivity and psychopathic trait scores. Although we found several associations, primarily positive in direction and involving frontal regions, the SMA and the caudate, there was no overlap of these regions with the regions selected for graph theoretical ROI analyses based on the networks implicated in the IIT. This makes it difficult to reconcile findings from the two types of analyses, yet it also highlights the importance of investigating presumed network abnormalities at a true network level, as done when using graph theory. Structural and functional abnormalities of both the SMA and caudate are recurrent findings in antisocial populations (83, 90, 93, 94). Caudal abnormalities are implicated in the non-

differentiation between reward and non-reward that underlies perseverance errors (95). SMA abnormalities are likely associated with low empathy that distinguishes psychopathy from antisocial behavior (90, 96). Importantly, since the current study measured resting-state activity, no inferences can be drawn regarding the functional roles played by the inter-region connectivity abnormalities that were identified.

4.1. Strengths and limitations

Strengths of the study include a large sample of females assessed for psychopathic traits using structured interviews (not self-reports), who presented a range of total and factor scores. While the PCL-R has not been psychometrically validated specifically for use with females nor with non-offender samples, a confirmatory factor analysis indicated no signs of measurement error. Further, thorough clinical assessments using a structured, validated diagnostic interview were available for all participants. Consequently, unlike previous studies that did not take account of mental disorders (28) or that recruited samples that were unrepresentative of clinical cases in that they presented no comorbid mental disorders (29, 30), the present investigation adjusted all analyses for current alcohol and drug dependence, anxiety and depression, psychoactive medication, and IQ. Future studies with large sample sizes are needed to disentangle the neural correlates of each of the covariates. This could be best achieved by prospective, longitudinal studies initiated in early childhood that involve both repeated brain scans and clinical assessments so as to identify neural alterations as disorders onset or traumas occur. Brain scans and clinical assessments need to be completed both before and after the onset of substance use.

Graph theoretical analyses of neuroimaging data have several limitations. One important limitation is the selection of nodes. In the current study, nodes were defined according to the well-established AAL atlas, the ROIs of which correspond to anatomically distinct structures (e.g. specific cortical gyri or subcortical structures), aiding interpretation of findings and allowing for comparison with past neuroimaging research of specific structures. A limitation of this approach is that a perfect overlap between the atlas mask and the actual center of neural activity cannot

be guaranteed. An alternative approach would be to select nodes based on empirically derived resting-state activity (97). Limitations of this latter approach include difficulty interpreting regional findings in light of the extant literature on specific structures, and an increased number of nodes, resulting in reduced statistical power to detect associations, after correction for multiple comparisons. Another limitation pertains to topology construction. Since the selection of a threshold is arbitrary, we investigated and reported associations across several different thresholds, considered only associations that were significant at two levels or more, and also investigated associations with non-thresholded networks. The choice of how to handle negative correlations between nodes is also arbitrary, since there is as of yet no plausible biological explanation for these (68). Finally, longitudinal topology data will be required to test whether specific topology abnormalities are in fact compensatory.

4.2. Conclusions

This is the first study to test IIT predictions of abnormal neural network topology among women and measuring psychopathic traits as dimensions. Findings suggest that psychopathic traits are associated with abnormal organization of the functional connectome, in partial support of predictions made by the IIT. Although no global topology abnormalities were found, specific nodes (regions), both hubs and non-hubs, showed abnormal topological properties, suggesting regional organizational abnormalities that were compensated for on a global level. The regional abnormalities may subservise lower order mechanisms (information processing and learning) that in turn are associated with psychopathic traits. Findings were robust to adjustment for IQ, anxiety, depression, substance dependence, and medication.

Acknowledgments

We express our gratitude to the young women who participated in the study. This study was conducted with a grant from MOBilisering mot narkotika (Swedish National Drug Policy Coordinator) and funds from the Stockholm County Council. PL, MB and JT are supported by a grant from the Swedish Foundation for Strategic Research; SH by a grant from the Stockholm County Council; JJ by grants from the Swedish Research Council and the Regional Agreement on

Medical Training and Clinical Research between the Stockholm County Council and Karolinska Institutet; IS by a grant from VINNOVA.

Financial disclosures

Author JT reports personal fees from the Finnish Medicines Agency (Fimea), European Medicines Agency (EMA), AstraZeneca, Bristol-Myers Squibb, Eli Lilly, F Hoffman-La Roche, GlaxoSmithKline, Janssen-Cilag, Lundbeck, Novartis, Organon, Otsuka, and Pfizer; and has received grants from the Stanley Foundation, Sigrid Jusélius Foundation, Eli Lilly, and Janssen-Cilag. The remaining authors report no biomedical financial interests or potential conflicts of interest.

References

1. Hare RD (2003): *The Hare Psychopathy Checklist-Revised*, 2nd ed. Toronto Multihealth Syst. Toronto: Multi-Health Systems.
2. Guay J-P, Ruscio J, Knight RA, Hare RD (2007): A taxometric analysis of the latent structure of psychopathy: evidence for dimensionality. *J Abnorm Psychol.* 116: 701–16.
3. Hyde LW, Shaw DS, Gardner F, Cheong J, Dishion TJ, Wilson M (2013): Dimensions of callousness in early childhood: Links to problem behavior and family intervention effectiveness. *Dev Psychopathol.* 25: 347–363.
4. Waller R, Dishion TJ, Shaw DS, Gardner F, Wilson MN, Hyde LW (2016): Does early childhood callous-unemotional behavior uniquely predict behavior problems or callous-unemotional behavior in late childhood? *Dev Psychol.* 52: 1805–1819.
5. Hemphälä M, Kosson D, Westerman J, Hodgins S (2015): Stability and predictors of psychopathic traits from mid-adolescence through early adulthood. *Scand J Psychol.* 56: 649–658.
6. Hemphälä M, Hodgins S (2014): Do psychopathic traits assessed in mid-adolescence predict mental health, psychosocial, and antisocial, including criminal outcomes, over the subsequent 5 years? *Can J Psychiatry.* 59: 40–9.
7. McMahon RJ, Witkiewitz K, Kotler JS (2010): Predictive validity of callous–unemotional traits measured in early adolescence with respect to multiple antisocial outcomes. *J Abnorm Psychol.* 119: 752–763.
8. Loney BR, Huntentburg A, Counts-Allan C, Schmeelk KM (2007): A preliminary examination of the intergenerational continuity of maternal psychopathic features. *Aggress Behav.* 33: 14–25.
9. Jaffee SR, Belsky J, Harrington H, Caspi A, Moffitt TE (2006): When parents have a history of conduct disorder: how is the caregiving environment affected? *J Abnorm Psychol.* 115: 309–19.
10. Larsson H, Andershed H, Lichtenstein P (2006): A genetic factor explains most of the

- variation in the psychopathic personality. *J Abnorm Psychol.* 115: 221–230.
11. Beaver KM, da Silva Costa C, Poersch AP, Freddi MC, Stelmach MC, Connolly EJ, Schwartz JA (2014): Psychopathic personality traits and their influence on parenting quality: results from a nationally representative sample of Americans. *Psychiatr Q.* 85: 497–511.
 12. Cale EM, Lilienfeld SO (2002): Sex differences in psychopathy and antisocial personality disorder. *Clin Psychol Rev.* 22: 1179–1207.
 13. Berkout O V., Young JN, Gross AM (2011): Mean girls and bad boys: Recent research on gender differences in conduct disorder. *Aggress Violent Behav.* 16: 503–511.
 14. Vitale JE, Smith SS, Brinkley C a., Newman JP (2002): The Reliability and Validity of the Psychopathy Checklist-Revised in a Sample of Female Offenders. *Crim Justice Behav.* 29: 202–231.
 15. Strand S, Belfrage H (2005): Gender differences in psychopathy in a Swedish offender sample. *Behav Sci Law.* 23: 837–50.
 16. De Brito S a., Hodgins S, Mccrory EJP, Mechelli a., Wilke M, Jones a. P, Viding E (2009): Structural Neuroimaging and the Antisocial Brain: Main Findings and Methodological Challenges. *Crim Justice Behav.* 36: 1173–1186.
 17. Kiehl K (2006): A cognitive neuroscience perspective on psychopathy: Evidence for paralimbic system dysfunction. *Psychiatry Res.* 142: 107–128.
 18. Seara-Cardoso A, Viding E (2014): Functional Neuroscience of Psychopathic Personality in Adults. *J Pers.* 1–15.
 19. Carré JM, Hyde LW, Neumann CS, Viding E, Hariri AR (2013): The neural signatures of distinct psychopathic traits. *Soc Neurosci.* 8: 122–35.
 20. Zhang J, Gao J, Shi H, Huang B, Wang X, Situ W, *et al.* (2014): Sex differences of uncinate fasciculus structural connectivity in individuals with conduct disorder. *Biomed Res Int.* 2014: 673165.
 21. Hamilton RKB, Hiatt Racer K, Newman JP (2015): Impaired integration in psychopathy: A unified theory of psychopathic dysfunction. *Psychol Rev.* 122: 770–791.

22. Bullmore E, Sporns O (2009): Complex brain networks: graph theoretical analysis of structural and functional systems. *Nat Rev Neurosci.* 10: 186–98.
23. van den Heuvel MP, Sporns O (2013): Network hubs in the human brain. *Trends Cogn Sci.* 17: 683–696.
24. Stevens A a, Tappon SC, Garg A, Fair D a (2012): Functional brain network modularity captures inter- and intra-individual variation in working memory capacity. *PLoS One.* 7: e30468.
25. Arnold AEGF, Protzner AB, Bray S, Levy RM, Iaria G (2014): Neural Network Configuration and Efficiency Underlies Individual Differences in Spatial Orientation Ability. *J Cogn Neurosci.* 26: 380–394.
26. Beaty RE, Kaufman SB, Benedek M, Jung RE, Kenett YN, Jauk E, *et al.* (2016): Personality and complex brain networks: The role of openness to experience in default network efficiency. *Hum Brain Mapp.* 37: 773–779.
27. Langer N, Pedroni A, Gianotti LRR, Hänggi J, Knoch D, Jäncke L (2012): Functional brain network efficiency predicts intelligence. *Hum Brain Mapp.* 33: 1393–406.
28. Yang Y, Raine A, Joshi A a, Joshi S, Chang Y-T, Schug R a, *et al.* (2012): Frontal information flow and connectivity in psychopathy. *Br J Psychiatry.* 201: 408–9.
29. Jiang Y, Liu W, Ming Q, Gao Y, Ma R, Zhang X, *et al.* (2016): Disrupted Topological Patterns of Large-Scale Network in Conduct Disorder. *Sci Rep.* 6: 37053.
30. Jiang W, Shi F, Liao J, Liu H, Wang T, Shen C, *et al.* (2016): Disrupted functional connectome in antisocial personality disorder. *Brain Imaging Behav.* 1–14.
31. Haney-Caron E, Caprihan A, Stevens MC (2014): DTI-measured white matter abnormalities in adolescents with Conduct Disorder. *J Psychiatr Res.* 48: 111–20.
32. Zhang J, Zhu X, Wang X, Gao J, Shi H, Huang B, *et al.* (2014): Increased structural connectivity in corpus callosum in adolescent males with conduct disorder. *J Am Acad Child Adolesc Psychiatry.* 53: 466–475.e1.
33. Sundram F, Deeley Q, Sarkar S, Daly E, Latham R, Craig M, *et al.* (2012): White matter

- microstructural abnormalities in the frontal lobe of adults with antisocial personality disorder. *Cortex*. 48: 216–29.
34. Lindner P, Savic I, Sitnikov R, Budhiraja M, Liu Y, Jokinen J, *et al.* (2016): Conduct disorder in females is associated with reduced corpus callosum structural integrity independent of comorbid disorders and exposure to maltreatment. *Transl Psychiatry*. 6: e714.
35. Menks WM, Furger R, Lenz C, Fehlbaum LV, Stadler C, Raschle NM (2016): Microstructural White Matter Alterations in the Corpus Callosum of Girls With Conduct Disorder. *J Am Acad Child Adolesc Psychiatry*. 4: 23–35.
36. Passamonti L, Fairchild G, Fornito A, Goodyer IM, Nimmo-Smith I, Hagan CC, Calder AJ (2012): Abnormal anatomical connectivity between the amygdala and orbitofrontal cortex in conduct disorder. (G. A. de Erausquin, editor) *PLoS One*. 7: e48789.
37. Sarkar S, Craig MC, Catani M, Dell’acqua F, Fahy T, Deeley Q, Murphy DGM (2013): Frontotemporal white-matter microstructural abnormalities in adolescents with conduct disorder: a diffusion tensor imaging study. *Psychol Med*. 43: 401–11.
38. Craig MC, Catani M, Deeley Q, Latham R, Daly E, Kanaan R, *et al.* (2009): Altered connections on the road to psychopathy. *Mol Psychiatry*. 14: 946–53, 907.
39. Motzkin JC, Newman JP, Kiehl K a, Koenigs M (2011): Reduced prefrontal connectivity in psychopathy. *J Neurosci*. 31: 17348–57.
40. Hoppenbrouwers SS, Nazeri A, de Jesus DR, Stirpe T, Felsky D, Schutter DJLG, *et al.* (2013): White matter deficits in psychopathic offenders and correlation with factor structure. *PLoS One*. 8: e72375.
41. Wolf RC, Pujara MS, Motzkin JC, Newman JP, Kiehl K a, Decety J, *et al.* (2015): Interpersonal traits of psychopathy linked to reduced integrity of the uncinate fasciculus. *Hum Brain Mapp*. 36: 4202–9.
42. Sobhani M, Baker L, Martins B, Tuvblad C, Aziz-Zadeh L (2015): Psychopathic traits modulate microstructural integrity of right uncinate fasciculus in a community population. *NeuroImage Clin*. 8: 32–38.

43. Breeden a L, Cardinale EM, Lozier LM, VanMeter JW, Marsh a a (2015): Callous-unemotional traits drive reduced white-matter integrity in youths with conduct problems. *Psychol Med.* 45: 3033–46.
44. Cohn MD, Pape LE, Schmaal L, van den Brink W, van Wingen G, Vermeiren RRJM, *et al.* (2015): Differential relations between juvenile psychopathic traits and resting state network connectivity. *Hum Brain Mapp.* 0. doi: 10.1002/hbm.22779.
45. Decety J, Yoder KJ, Lahey BB (2015): Sex differences in abnormal white matter development associated with conduct disorder in children. *Psychiatry Res - Neuroimaging.* 233: 269–277.
46. Sarkar S, Dell’Acqua F, Froudust Walsh S, Blackwood N, Scott S, Craig MC, *et al.* (2016): A Whole-Brain Investigation of White Matter Microstructure in Adolescents with Conduct Disorder. (P.-T. Yap, editor) *PLoS One.* 11: e0155475.
47. Pape LE, Cohn MD, Caan MWA, van Wingen G, van den Brink W, Veltman DJ, Popma A (2015): Psychopathic traits in adolescents are associated with higher structural connectivity. *Psychiatry Res Neuroimaging.* 233: 474–480.
48. Walters GD, Ermer E, Knight RA, Kiehl KA (2015): Paralimbic biomarkers in taxometric analyses of psychopathy: does changing the indicators change the conclusion? *Personal Disord.* 6: 41–52.
49. Satterthwaite TD, Wolf DH, Roalf DR, Ruparel K, Erus G, Vandekar S, *et al.* (2015): Linked Sex Differences in Cognition and Functional Connectivity in Youth. *Cereb Cortex.* 25: 2383–94.
50. Ingahlalkar M, Smith A, Parker D, Satterthwaite TD, Elliott M a, Ruparel K, *et al.* (2014): Sex differences in the structural connectome of the human brain. *Proc Natl Acad Sci U S A.* 111: 823–8.
51. Smith SS, Newman JP (1990): Alcohol and drug abuse-dependence disorders in psychopathic and nonpsychopathic criminal offenders. *J Abnorm Psychol.* 99: 430–9.
52. Skeem J, Johansson P, Andershed H, Kerr M, Louden JE (2007): Two subtypes of psychopathic violent offenders that parallel primary and secondary variants. *J Abnorm Psychol.* 116: 395–409.

53. Willemsen J, Vanheule S, Verhaeghe P (2011): Psychopathy and lifetime experiences of depression. *Crim Behav Ment Heal*. 21: 279–294.
54. Modi S, Kumar M, Kumar P, Khushu S (2015): Aberrant functional connectivity of resting state networks associated with trait anxiety. *Psychiatry Res - Neuroimaging*. 234: 25–34.
55. Zhu X, Cortes CR, Mathur K, Tomasi D, Momenan R (2017): Model-free functional connectivity and impulsivity correlates of alcohol dependence: a resting-state study. *Addict Biol*. 22: 206–217.
56. Palmer SM, Crewther SG, Carey LM (2015): A Meta-Analysis of Changes in Brain Activity in Clinical Depression. *Front Hum Neurosci*. 8. doi: 10.3389/fnhum.2014.01045.
57. Hodgins S, Tengström A, Bylin S, Göranson M, Hagen L, Janson M, *et al.* (2007): Consulting for substance abuse: mental disorders among adolescents and their parents. *Nord J Psychiatry*. 61: 379–86.
58. Hodgins S, Oliver BR, Tengström A, Larsson A (2010): Adolescents who consulted for substance misuse problems: outcomes 1 year later. *Nord J Psychiatry*. 64: 189–95.
59. Hodgins S, Lövenhag S, Rehn M, Nilsson KW (2014): A 5-year follow-up study of adolescents who sought treatment for substance misuse in Sweden. *Eur Child Adolesc Psychiatry*. 23: 347–60.
60. Budhiraja M, Savic I, Lindner P, Jokinen J, Tiihonen J, Hodgins S (2017): Brain structure abnormalities in young women who presented conduct disorder in childhood/adolescence. *Cogn Affect Behav Neurosci*. 17: 869–885.
61. Lindner P, Budhiraja M, Westerman J, Savic I, Jokinen J, Tiihonen J, Hodgins S (2017): White matter correlates of psychopathic traits in a female community sample. *Soc Cogn Affect Neurosci*. 12: 1500–1510.
62. First MB, Spitzer RL, Miriam G, Williams JBW (2002): *Structured Clinical Interview for DSM-IV-TR Axis I Disorders, Research Version, Patient Edition (SCID-I/P)*. New York: Biometrics Research, New York State Psychiatric Institute.
63. Coid J, Yang M, Ullrich S, Roberts A, Hare RD (2009): Prevalence and correlates of

- psychopathic traits in the household population of Great Britain. *Int J Law Psychiatry*. 32: 65–73.
64. Cooke DJ, Michie C (1999): Psychopathy across cultures: North America and Scotland compared. *J Abnorm Psychol*. 108: 58–68.
65. Whitfield-Gabrieli S, Nieto-Castanon A (2012): Conn: a functional connectivity toolbox for correlated and anticorrelated brain networks. *Brain Connect*. 2: 125–41.
66. Tzourio-Mazoyer N, Landeau B, Papathanassiou D, Crivello F, Etard O, Delcroix N, *et al.* (2002): Automated Anatomical Labeling of Activations in SPM Using a Macroscopic Anatomical Parcellation of the MNI MRI Single-Subject Brain. *Neuroimage*. 15: 273–289.
67. Kruschwitz JD, List D, Waller L, Rubinov M, Walter H (2015): GraphVar: A user-friendly toolbox for comprehensive graph analyses of functional brain connectivity. *J Neurosci Methods*. 245: 107–115.
68. Rubinov M, Sporns O (2010): Complex network measures of brain connectivity: uses and interpretations. *Neuroimage*. 52: 1059–69.
69. Menon V, Uddin LQ (2010): Saliency, switching, attention and control: a network model of insula function. *Brain Struct Funct*. 1–13.
70. Baskin-Sommers AR, Curtin JJ, Newman JP (2015): Altering the Cognitive-Affective Dysfunctions of Psychopathic and Externalizing Offender Subtypes With Cognitive Remediation. *Clin Psychol Sci*. 3: 45–57.
71. Vieira JB, Ferreira-Santos F, Almeida PR, Barbosa F, Marques-Teixeira J, Marsh AA (2014): Psychopathic traits are associated with cortical and subcortical volume alterations in healthy individuals. *Soc Cogn Affect Neurosci*. 10: 1693–1704.
72. Juárez M, Kiehl K a, Calhoun VD (2013): Intrinsic limbic and paralimbic networks are associated with criminal psychopathy. *Hum Brain Mapp*. 34: 1921–30.
73. Broulidakis MJ, Fairchild G, Sully K, Blumensath T, Darekar A, Sonuga-Barke EJS (2016): Reduced Default Mode Connectivity in Adolescents With Conduct Disorder. *J Am Acad Child Adolesc Psychiatry*. 55: 800–808.e1.

74. Broyd SJ, Demanuele C, Debener S, Helps SK, James CJ, Sonuga-Barke EJS (2009): Default-mode brain dysfunction in mental disorders: a systematic review. *Neurosci Biobehav Rev.* 33: 279–96.
75. Whitfield-Gabrieli S, Ford JM (2012): Default mode network activity and connectivity in psychopathology. *Annu Rev Clin Psychol.* 8: 49–76.
76. Freeman SM, Clewett D V, Bennett CM, Kiehl K a, Gazzaniga MS, Miller MB (2014): The Posteromedial Region of the Default Mode Network Shows Attenuated Task-Induced Deactivation in Psychopathic Prisoners. *Neuropsychology.* 29: 493–500.
77. Kennedy DP, Redcay E, Courchesne E (2006): Failing to deactivate: Resting functional abnormalities in autism. *Proc Natl Acad Sci.* 103: 8275–8280.
78. Lozier LM, Cardinale EM, VanMeter JW, Marsh A a (2014): Mediation of the relationship between callous-unemotional traits and proactive aggression by amygdala response to fear among children with conduct problems. *JAMA psychiatry.* 71: 627–36.
79. Sebastian CL, McCrory EJP, Cecil C a M, Lockwood PL, De Brito S a, Fontaine NMG, Viding E (2012): Neural responses to affective and cognitive theory of mind in children with conduct problems and varying levels of callous-unemotional traits. *Arch Gen Psychiatry.* 69: 814–22.
80. Hyde LW, Byrd AL, Votruba-Drzal E, Hariri AR, Manuck SB (2014): Amygdala reactivity and negative emotionality: divergent correlates of antisocial personality and psychopathy traits in a community sample. *J Abnorm Psychol.* 123: 214–24.
81. Boccardi M, Ganzola R, Rossi R, Sabbatoli F, Laakso MP, Repo-Tiihonen E, *et al.* (2010): Abnormal hippocampal shape in offenders with psychopathy. *Hum Brain Mapp.* 31: 438–47.
82. Laakso MP, Vaurio O, Koivisto E, Savolainen L, Eronen M, Aronen HJ, *et al.* (2001): Psychopathy and the posterior hippocampus. *Behav Brain Res.* 118: 187–93.
83. Alegria AA, Radua J, Rubia K (2016): Meta-Analysis of fMRI Studies of Disruptive Behavior Disorders. *Am J Psychiatry.* 173: 1119–1130.
84. Newman JP, Kosson DS (1986): Passive avoidance learning in psychopathic and nonpsychopathic offenders. *J Abnorm Psychol.* 95: 252–256.

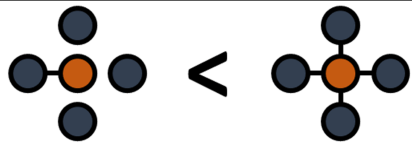

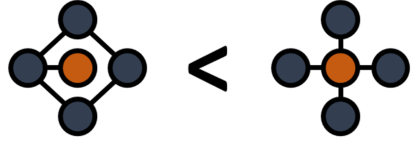
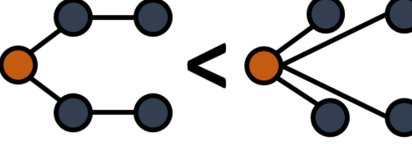
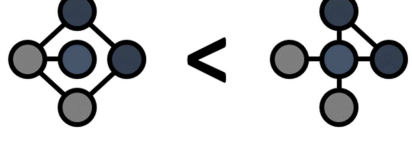
85. Budhani S, Richell R a, Blair RJR (2006): Impaired reversal but intact acquisition: probabilistic response reversal deficits in adult individuals with psychopathy. *J Abnorm Psychol.* 115: 552–558.
86. Rogers JC, Brito SA De (2015): Cortical and Subcortical Gray Matter Volume in Youths With Conduct Problems A Meta-analysis. *JAMA psychiatry.* i: 1–9.
87. Gregory S, Ffytche D, Simmons A, Kumari V, Howard M, Hodgins S, Blackwood N (2012): The antisocial brain: psychopathy matters. *Arch Gen Psychiatry.* 69: 962–72.
88. Ermer E, Cope LM, Nyalakanti PK, Calhoun VD, Kiehl K a (2013): Aberrant paralimbic gray matter in incarcerated male adolescents with psychopathic traits. *J Am Acad Child Adolesc Psychiatry.* 52: 94–103.e3.
89. Birbaumer N, Veit R, Lotze M, Erb M, Hermann C, Grodd W, Flor H (2005): Deficient fear conditioning in psychopathy: a functional magnetic resonance imaging study. *Arch Gen Psychiatry.* 62: 799–805.
90. Decety J, Skelly LR, Kiehl K a (2013): Brain response to empathy-eliciting scenarios involving pain in incarcerated individuals with psychopathy. *JAMA Psychiatry.* 70: 638–45.
91. Gregory S, Blair RJ, fytche D, Simmons A, Kumari V, Hodgins S, Blackwood N (2015): Punishment and psychopathy: A case-control functional MRI investigation of reinforcement learning in violent antisocial personality disordered men. *The Lancet Psychiatry.* 2: 153–160.
92. Singer T, Critchley HD, Preuschoff K (2009): A common role of insula in feelings, empathy and uncertainty. *Trends Cogn Sci.* 13: 334–340.
93. Fairchild G, Passamonti L, Hurford G, Hagan CC, von dem Hagen E a H, van Goozen SHM, *et al.* (2011): Brain structure abnormalities in early-onset and adolescent-onset conduct disorder. *Am J Psychiatry.* 168: 624–33.
94. Hyatt CJ, Haney-Caron E, Stevens MC (2012): Cortical thickness and folding deficits in conduct-disordered adolescents. *Biol Psychiatry.* 72: 207–14.
95. Glenn AL, Yang Y (2012): The potential role of the striatum in antisocial behavior and

psychopathy. *Biol Psychiatry*. 72: 817–22.

96. Decety J, Michalska KJ, Akitsuki Y, Lahey BB (2009): Atypical empathic responses in adolescents with aggressive conduct disorder: a functional MRI investigation. *Biol Psychol*. 80: 203–11.

97. Power JD, Cohen AL, Nelson SM, Wig GS, Barnes KA, Church JA, *et al.* (2011): Functional Network Organization of the Human Brain. *Neuron*. 72: 665–678.

Table 1. Investigated graph theory measures of network topology

Measures	Level	Details	Illustration
Degree	Local	Number of edges of a node.	 The illustration shows two nodes, each with a central orange node and four surrounding blue nodes. The left node has four edges connecting it to the surrounding nodes, while the right node has five edges connecting it to the surrounding nodes. A greater-than sign (>) is placed between them.
Strength	Local	Sum of weighted edges of a node.	 The illustration shows two nodes, each with a central orange node and one surrounding blue node. The left node has a thin edge connecting them, while the right node has a thick edge connecting them. A greater-than sign (>) is placed between them.
Betweenness centrality	Local	Fraction of all shortest paths in the network that pass through a node.	 The illustration shows two nodes, each with a central orange node and four surrounding blue nodes. The left node is part of a diamond-shaped network where it is a central hub, while the right node is part of a star-shaped network where it is the central hub. A greater-than sign (>) is placed between them.
Efficiency	Local and Global	Inverse shortest path length.	 The illustration shows two nodes, each with a central orange node and four surrounding blue nodes. The left node is part of a network where it is a hub, while the right node is part of a network where it is a leaf. A greater-than sign (>) is placed between them.
Clustering coefficient	Global	Percentage of fully connected triplets (three connected nodes) divided by the total number of triplets.	 The illustration shows two nodes, each with a central orange node and four surrounding blue nodes. The left node is part of a network where it is a hub, while the right node is part of a network where it is a leaf. A greater-than sign (>) is placed between them.

Running title: Psychopathy and network topology

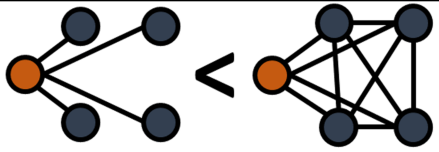
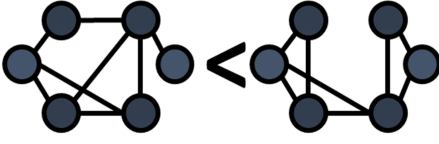
Characteristic path length	Global	Average number of steps along the shortest path between all possible pairs of nodes.	
Modularity	Global	Scaled Louvain modularity: density of edges inside communities compared to edges outside communities.	

Table 2. Significant associations of psychopathy total and factor scores with inter-region connectivity

Predictor	Region #1	Region #2	Statistics
<i>Model: Connectivity ~ PCL total score</i>			
Total score	Right caudate	Right frontal middle gyrus	B=0.41, t=3.83, p=.000270
Total score	Right caudate	Left rectus	B=0.41, t=3.76, p=.000342
Total score	Left SMA	Right rectus	B=.40, t=3.69, p=.000438
Total score	Left superior temporal pole	Right paracentral lobule	B=-.41, t=-3.73, p=.000380
<i>Model: Connectivity ~ PCL Factor 1 + Factor 2 scores</i>			
Factor 2	Left SMA	Left rectus	B=0.65, t=4.00, p=.000154
Factor 2	Left SMA	Right rectus	B=0.62, t=3.80, p=.000303

Standardized beta values reported. All associations survived False Discovery Rate (FDR) correction.

Figure 1. Distribution of psychopathy scores

[Figure attached separately]

ACCEPTED MANUSCRIPT

Figure 2. Regions of interest and presumed topology

[Figure attached separately]

Raw topology; not spatially accurate. Region abbreviations: MFG, Middle Frontal Gyrus; dlPFC, rostralateral prefrontal cortex; mPFC, medial prefrontal cortex; IPL, inferior parietal lobe; ACC, anterior cingulate cortex; TPJ, temporo-parietal junction; PCC, posterior cingulate cortex; vlPFC, ventrolateral prefrontal cortex. Network abbreviations: CoN, Cingulo-opercular Network; DMN, Default Mode Network; FpCN, Frontoparietal Control Network; VAN, Ventral Attention Network.

Figure 3. Significant associations of psychopathy total and factor scores with inter-region connectivity

[Figure attached separately]

Color of edge according to direction (positive: blue, negative: red) of association with psychopathy measure. Thickness of edge according to strength of (relative) correlation. Associations between network measures and the Interpersonal-affective and Social deviance factor scores are adjusted for the other score. Associations with total score were investigated in a separate model. Abbreviations: CAU: caudate, REC: rectus, SMA: supplementary motor area, TPO: temporal pole, PCL: paracentral lobule, MFG: middle frontal gyrus.

Figure 4. Levels of significance of global topology associations with psychopathy scores

[Figure attached separately]

Associations between network measures and the Interpersonal-affective and Social deviance factor scores are adjusted for the other score. Associations with total score were investigated in a separate model.

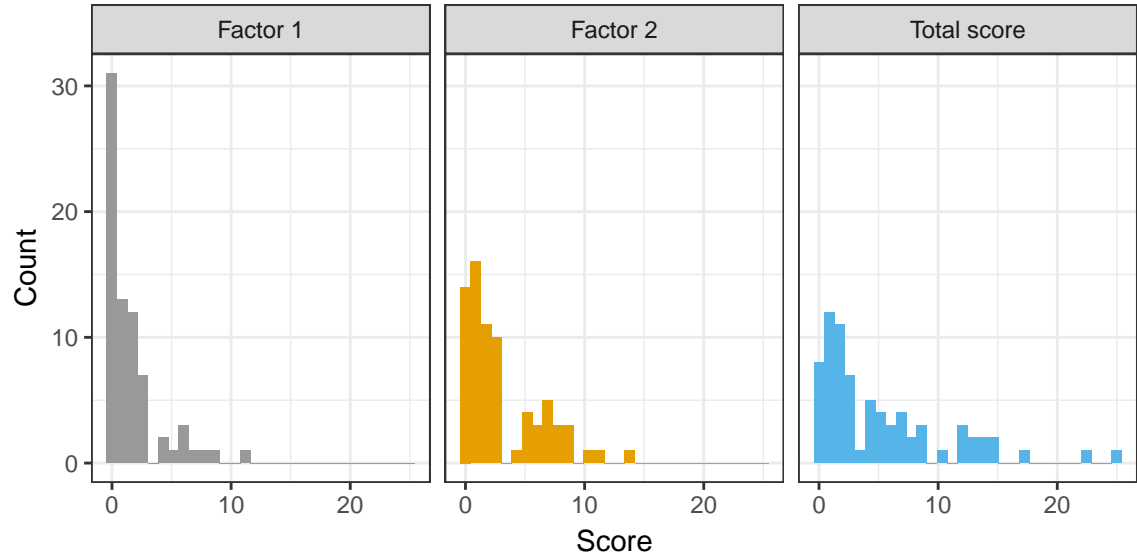
ACCEPTED MANUSCRIPT

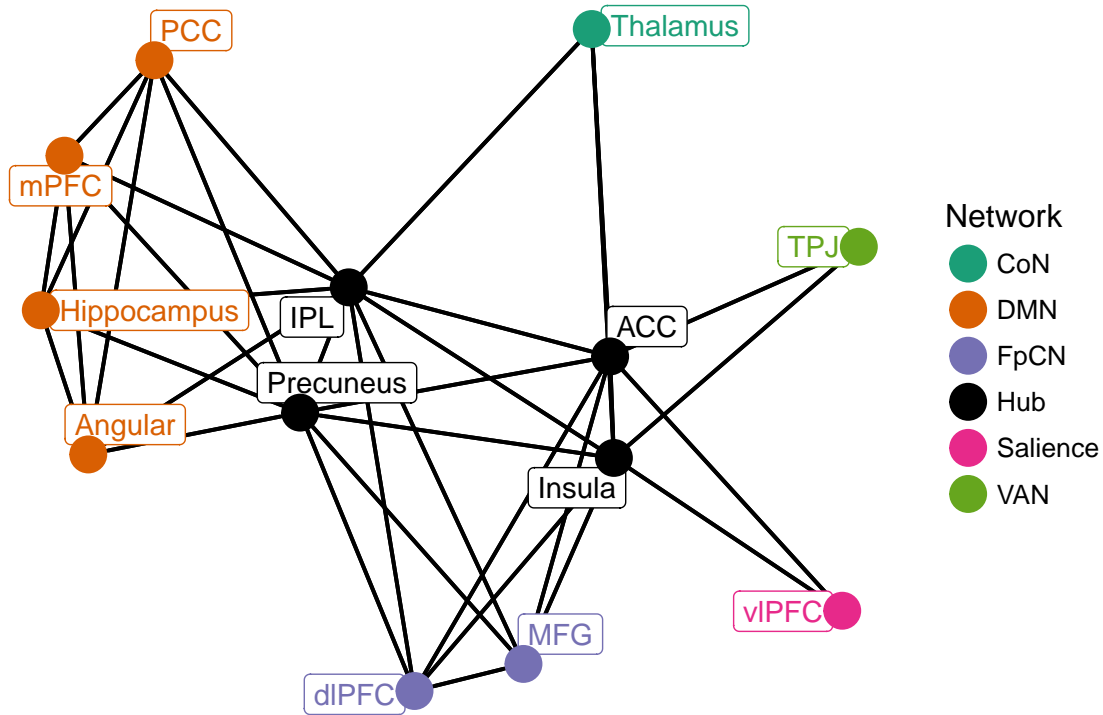
Figure 5. Levels of significance of local topology associations with psychopathy scores

[Figure attached separately]

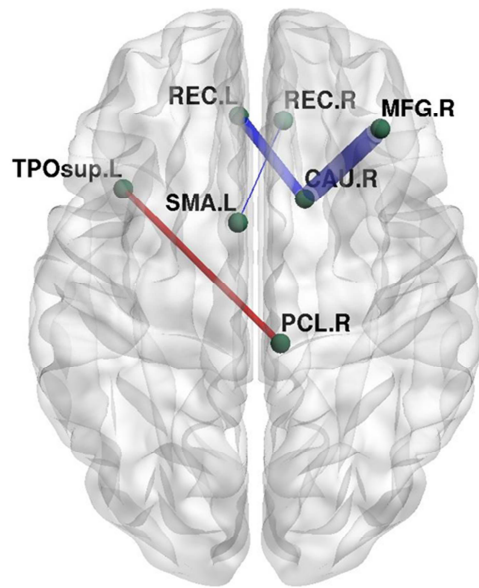
Associations between network measures and the Interpersonal-affective and Social deviance factor scores are adjusted for the other score. Associations with total score were investigated in a separate model.

ACCEPTED MANUSCRIPT

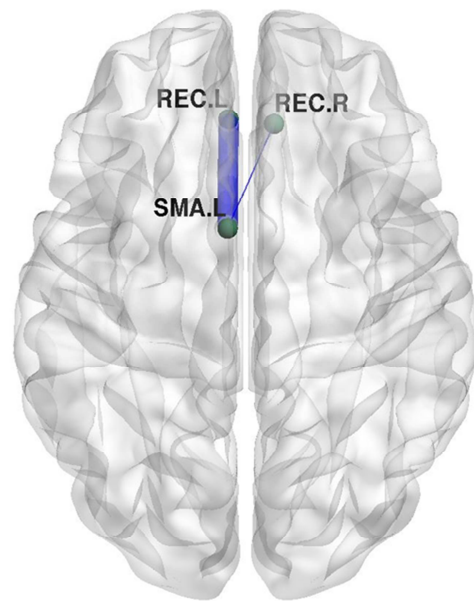




(A) Associations with total psychopathy scores

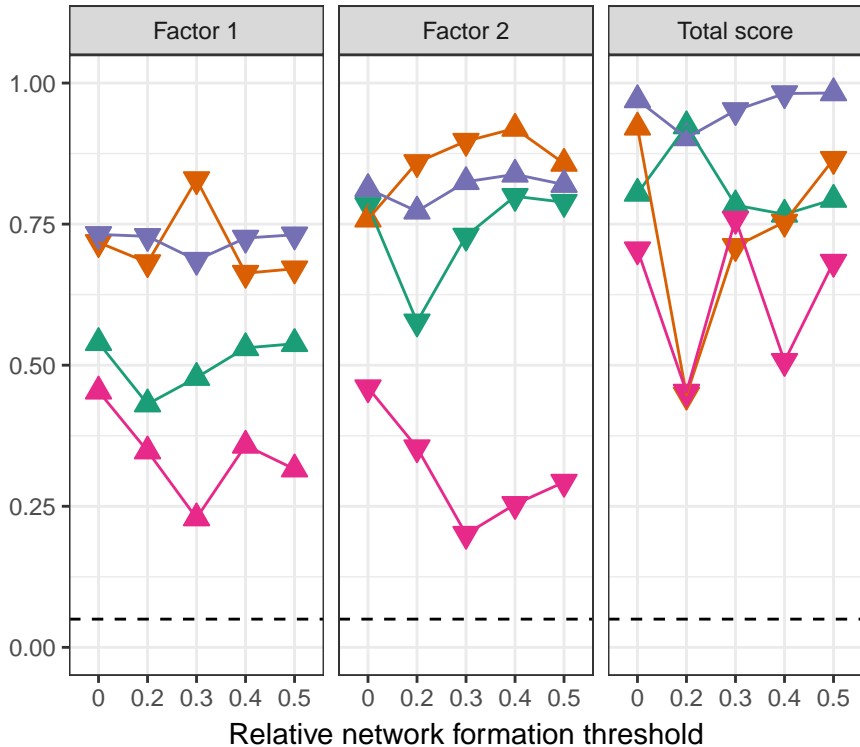


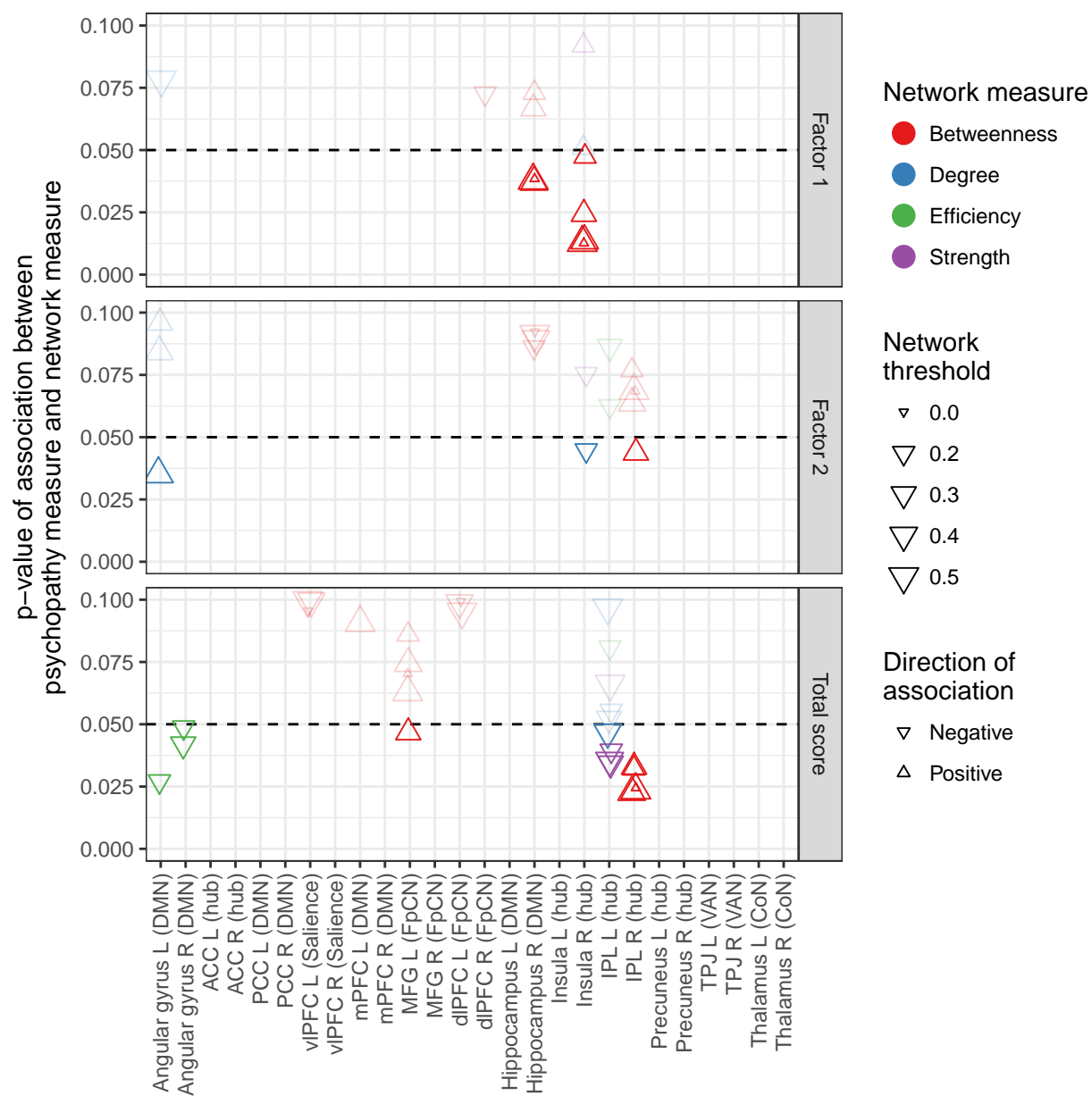
(B) Associations with Social Deviance (factor 2) score



ACCEPTED MANUSCRIPT

p-value of association between
psychopathy score and network measure





Associations of Psychopathic Traits With Local and Global Brain Network Topology in Young Adult Women

Supplemental Information

Supplementary Methods and Materials

Confirmatory factor analysis

To examine the construct validity of measuring psychopathic traits in a non-forensic sample using the PCL-R, confirmatory factor analysis (CFA) was performed using the *lavaan* R package (1). To maximize the sample size, important for CFA modeling and interpretation of some fit measures, all female ex-clients that participated in the previous assessment wave (when the PCL-R was administered) and provided complete data on an item-level ($n=79$) were included in the CFA. Although the two-factor solution was subsequently chosen to correlate psychopathy scores with brain connectivity metrics (in order to increase the score variation), the CFA modeled the four-facet, 1st order solution in which each factor consists of two facet (Interpersonal+Affective and Lifestyle+Antisocial) since this has been shown to be the best fitting solution and would enable comparisons with CFA results obtained in forensic samples (2). Item 19 (“Revocation of conditional release”) was omitted since there was no variation of scores in the sample. The hypothesized factor solution was modeled using maximum likelihood estimation by including four latent variables (facets), each manifested by a set of observed variables (items), featuring residual variance, correlations of exogenous variables and fixed factor loading of the first indicator of each latent variable.

Obtained standardized estimates of the model components are shown in Figure S1 below. Root Mean Square Error of Approximation (RMSEA) for the model was calculated to 0.087 (90% confidence interval: 0.063—0.110), the Standardized Root Mean Square Residual (SRMR) to 0.085, the Comparative Fit Index (CFI) to 0.853, and the Tucker-Lewis Index (TLI) to 0.823, indicative of adequate model fit considering the small ($n<250$) sample size (3).

MRI acquisition and preprocessing

Images were acquired using a 3-Tesla MRI scanner (MR750 GE Healthcare, Milwaukee, WI, USA) with an eight-channel array coil (in-Vivo, Gainesville, FL, USA). For co-registration with the functional images, high-resolution (1 mm³), fast-spoiled T1-weighted anatomical images were acquired in the axial plane with a 12° flip angle; echo time, 3.1 ms; repetition time, 7.9 ms; and 176 slices, for structural registration of fMRI data. Preprocessing steps included: slice timing correction, realignment to the mean image (motion correction), anatomical-functional co-registration, tissue segmentation, direct normalization into MNI space, and 8 mm Gaussian smoothing. Data were then band-pass filtered (0.008—0.09 Hz, after nuisance regression). Nuisance regressors included 6 realignment parameters, 5 principal components from white matter signals and CSF, respectively, using a principal component (PCA) based noise correction (CompCorr) approach. Additionally, volumes exceeding 0.5 mm frame wise displacement or 3 standard deviation global signal intensity change were regressed out.

Supplementary Table S1. Sample characteristics

Variable	Mean (SD) or frequency (%)
Verbal IQ	M=8.89 (SD=2.50)
Performance IQ	M=10.15 (SD=3.10)
Any current psychoactive medication	N=4 (5.5%)
Current alcohol dependence	N=0 (0%)
Current drug dependence	N=2 (2.7%)
Any current anxiety disorder	N=15 (20.5%)
Current depression	N=3 (4.1%)

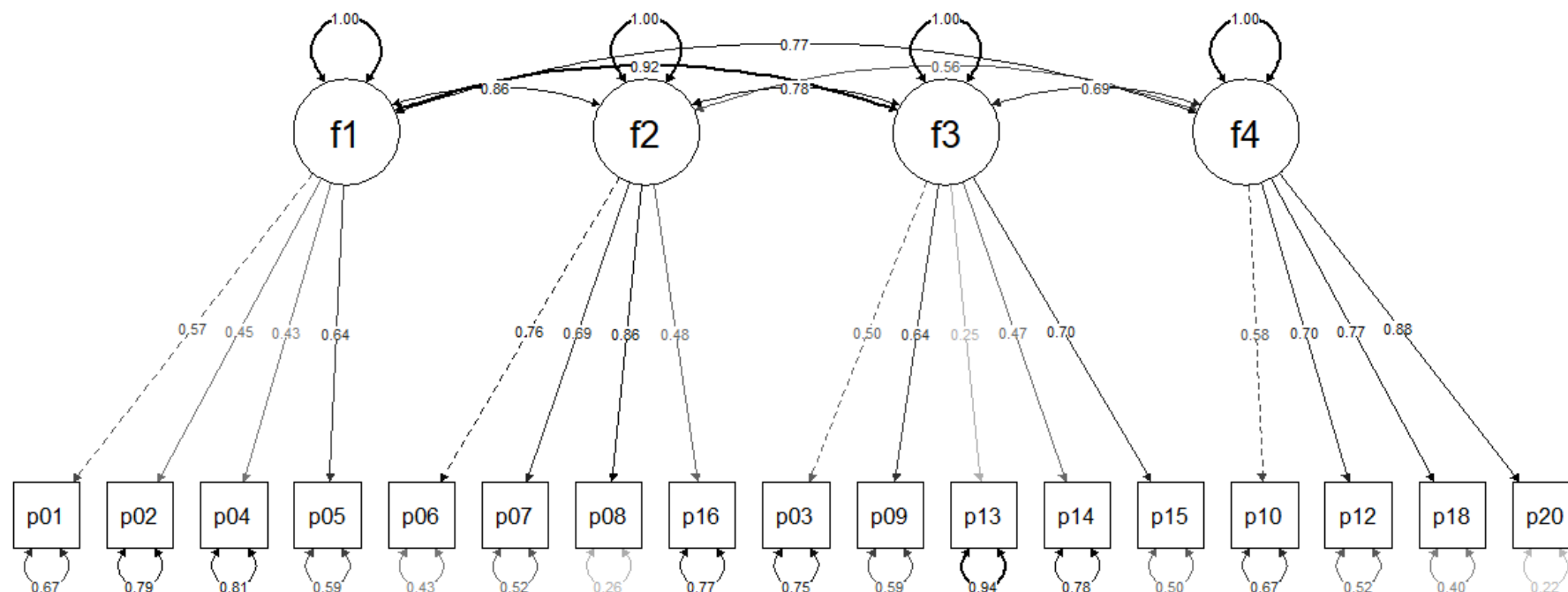
Supplementary Table S2. Results of regression analyses estimating associations of verbal and performance IQ and comorbid disorders with total psychopathy and factor scores

Predictor	Factor 1: Interpersonal-Affective			Factor 2: Social Deviance			Total score		
	B	SE	p	B	SE	p	B	SE	p
Verbal IQ	-0.23	0.11	0.04*	-0.38	0.15	0.01*	-0.59	0.25	.02*
Performance IQ	-0.09	0.09	0.33	-0.22	0.12	0.07	-0.31	0.21	.14
Any current psychoactive medication	0.61	1.22	0.62	1.51	1.62	0.36	1.73	2.79	.54
Current drug dependence	3.91	1.62	0.02*	4.98	2.23	0.03*	8.51	3.76	.03*
Any current anxiety disorder	1.39	0.66	0.04*	0.39	0.93	0.68	1.9	1.56	.23
Current depression	1.01	1.38	0.47	0.88	1.89	0.64	2.55	3.19	.43

Current alcohol dependence was assessed but no participant met criteria.

Supplementary Table S3. Atlas regions used as nodes

Node	AAL notation	Network
Angular Gyrus	Angular	Default Mode
Anterior Cingulate Cortex	Cingulum_Ant	Hub
Posterior Cingulate Cortex	Cingulum_Post	Default Mode
Ventrolateral PFC	Frontal_Inf_Orb	Saliency
Medial PFC	Frontal_Med_Orb	Default Mode
Middle Frontal Gyrus	Frontal_Mid	Fronto-parietal Control
Dorsolateral PFC	Frontal_Sup_Medial	Fronto-parietal Control
Hippocampus	Hippocampus	Default Mode
Insula	Insula	Hub
Inferior Parietal Lobe	Parietal_Inf	Hub
Precuneus	Precuneus	Hub
Temporo-Parietal Junction	Temporal_Mid	Ventral Attention
Thalamus	Thalamus	Cingulo-opercular



Supplementary Figure S1. Confirmatory factor analysis of four-facet solution showing standardized parameter estimates. Dashed lines indicate fixed factor loadings; other lines vary alpha by loading strength.

Abbreviations: f1=Interpersonal facet, f2=Affective facet, f3=Lifestyle facet, f4=Antisocial facet, p01=Glibness/superficial charm, p02=Grandiose sense of self-worth, p03=Stimulation seeking, p04=Pathological lying, p05=Conning/manipulative, p06=Lack of remorse/guilt, p07=Emotionally shallow, p08=Callous/lack of empathy, p09=Parasitic lifestyle, p10=Poor behavioral control, p12=Early behavioral problems, p13=Lack of goals, p14=Impulsivity, p15=Irresponsibility, p16=Failure to accept responsibility, p18=Juvenile delinquency, p20=Criminal versatility.

Supplemental References

1. Rosseel, Y. (2012). lavaan: An R Package for Structural Equation Modelin. *Journal of Statistical Software*, 48(2), 1–36. Retrieved from <http://www.jstatsoft.org/v48/i02/>
2. Hare, R. D., & Neumann, C. S. (2005). Structural models of psychopathy. *Current Psychiatry Reports*, 7(1), 57–64. <https://doi.org/10.1007/s11920-005-0026-3>
3. Hu, L. T., & Bentler, P. M. (1999). Cutoff criteria for fit indexes in covariance structure analysis: Conventional criteria versus new alternatives. *Structural Equation Modeling*, 6(1), 1–55. <https://doi.org/10.1080/10705519909540118>

ACCEPTED MANUSCRIPT